2016 International Symposium on Nonlinear Theory and Its Applications,
NOLTA2016, Yugawara, Japan, November 27th-30th, 2016

Stability of Paralleled Boost Converters with WTA Switching

Yasuo Murata† and Toshimichi Saito†

†Department of Electronics and Electrical Engineering, Hosei University
3–7–2 Kajino-cho, Koganei, Tokyo 184-8584, Japan
Emails: yasuo.murata.6c@stu.hosei.ac.jp; tsaito@hosei.ac.jp

Abstract—This paper studies a paralleled system of boost converters with WTA-based switching rule. The system exhibits multi-phase synchronization phenomena and chaotic phenomena. The multi-phase synchronization is suitable for ripple reduction, current sharing, and efficient power supply. The WTA-based switching rule is effective to reinforce the fault tolerance. Simplifying the system into a piecewise linear model, stability of the synchronization phenomena and ripple waveforms can be analyzed precisely.

1. Introduction

The paralleled systems of switching power converters have been studied from fundamental and application viewpoints. In the fundamental study, the paralleled systems are interesting examples of switched dynamical systems that can exhibit a variety of nonlinear phenomena such as multi-phase synchronization and chaos [1]-[4]. In the applications, the paralleled systems can realize current sharing and ripple reduction which are effective in robust and reliable power management [5]-[9]. In these studies, analysis of nonlinear phenomena is important and single power converters have been studied sufficiently. However, the analysis of the paralleled systems is not easy because they are higher dimensional nonlinear systems with various complex behavior.

This paper studies stability of a paralleled system of N boost converters through which N pieces of input voltage sources are applied to a load. The N boost converters are coupled by the winner-take-all (WTA) switching rule that can realize N-phase synchronization (N-SYN) automatically. The N-SYN is suitable for ripple reduction of input current that is effective to realize higher efficiency operation. Especially, if the input voltage is given by solar cells, the rippled reduction is well suited for maximum power point tracking [10] [11]. The parallel operation is also suitable in viewpoint of fault-tolerance: if some converter is broken, the other converters can preserve the operation. In order to analyze the system, we introduce a simple piecewise linear model and provide a sufficient condition of parameters for stability of N-SYN and precise calculation formula of the input ripple. These results can clarify stable operation, power efficiency and fault tolerance. Performing basic numerical experiments, the stability of N-SYN and robust operation of the circuit are confirmed. We have prepared laboratory measurements of typical phenomena for the final version.

2. 3-Paralleled Boost Converter

Fig. 1 shows the simplified circuit model of the paralleled boost converters where r_L is an inner resistance of inductor. The j-th converter includes the switch S_j and diode D_j which can be either of the State A or State B: where $j = 1 \sim N$.

$$\begin{array}{l}\text{State A: } S \text{ conducting, } D \text{ blocking, and } i_j > 0. \\ \text{State B: } S \text{ blocking, } D \text{ conducting, and } i_j > 0.\end{array} \quad (1)$$

For simplicity, let $N = 3$ hereafter. Let $i_{in} = i_1 + i_2 + i_3$ be an input current. In order to simplify the analysis, RC load is replaced with constant voltage sources V_{oj} shown in Fig. 3 where $RC \gg T$ is assumed. T is a clock period.

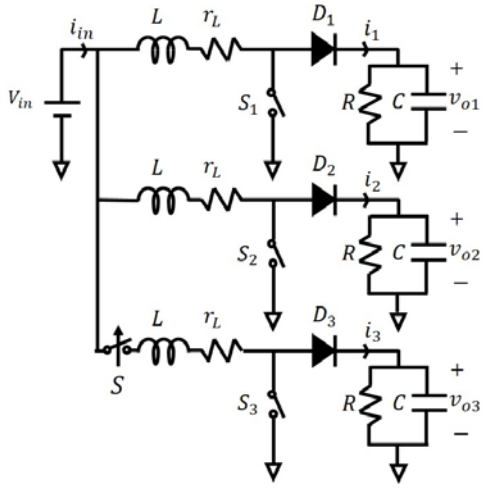

Figure 1: A circuit model of 3-paralleled boost converters.

This circuit dynamics is described by

$$\frac{Ldi_j}{dt} = \begin{cases} -r_L i_j + V_{in} & \text{for State A} \\ -r_L i_j + V_{in} - V_{oj} & \text{for State B} \end{cases} \quad (2)$$

Eq. (6) is changed into the following dimensionless equation because the analysis is simplified.

$$\frac{dx_j}{d\tau} = \begin{cases} -\gamma x_j + a & \text{for State A} \\ -\gamma x_j - b_j & \text{for State B} \end{cases} \quad (3)$$

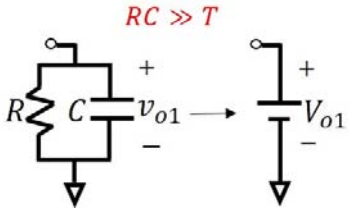

Figure 2: simplified model of RC load.

Where the following dimensionless variables and parameters are used:

$$a = \frac{TV_{in}}{LJ},\ b_j = \frac{T(V_{oj} - V_{in})}{LJ}\ \gamma_j = \frac{Tr_L}{L}$$
$$\tau = \frac{t}{T},\ x_j = \frac{i_j}{J},\ X_- = \frac{J_-}{J} \tag{4}$$

Let $x_{in} = i_{in}/J = x_1 + x_2 + x_3$ be a dimensionless input current. In the circuit, $J_- > 0$ is the lower current threshold and $J > 0$ is a current criterion for a desired operation. The state transition is defined by following switching rule. In the State A, the inductor current i_j rises as shown in Fig. 3. If the x_j is the maximum among x_1 to x_N at some clock signal arriving time $\tau = n$ then State A is changed into State B. Let the j-th system be State B where j-th dimensionless current x_j decays. If the x_j reaches the lower threshold X_- then the State B changed into State A. Note that the three converters are connected by the comparison of $x_1 \sim x_3$ ($i_1 \sim i_3$) in the SW rule.

$$\text{SW rule}\begin{cases} \text{State A} \rightarrow \text{State B if } i_j\text{=Max } (t = nT) \\ \text{State B} \rightarrow \text{State A if } i_j = J_- \end{cases} \tag{5}$$

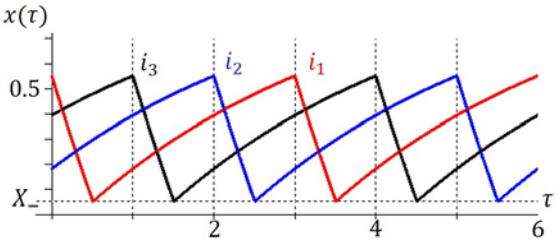

Figure 3: WTA switching rule

The piecewise exact solution is given by

$$x_j(\tau) = \begin{cases} (x(0) - \mathrm{a}/\gamma)e^{-\gamma\tau} + \mathrm{a}/\gamma & \text{for State A} \\ (x(0) + \mathrm{b_j}/\gamma)e^{-\gamma\tau} - \mathrm{b_j}/\gamma & \text{for State B} \end{cases} \tag{6}$$

If $Df_N(a, b)$ is larger than 1, the N-SYN is unstable where $x(0)$ indicates an initial value. Using these equations, we can calculate waveforms precisely. In this paper, the parameters condition is following.

$$a = 0.3,\ \gamma = 0.3,\ X_- = 0.05,\ b_j : \text{varies}$$

Fig. 4 shows typical waveforms of 3-phase synchronization phenomenon.

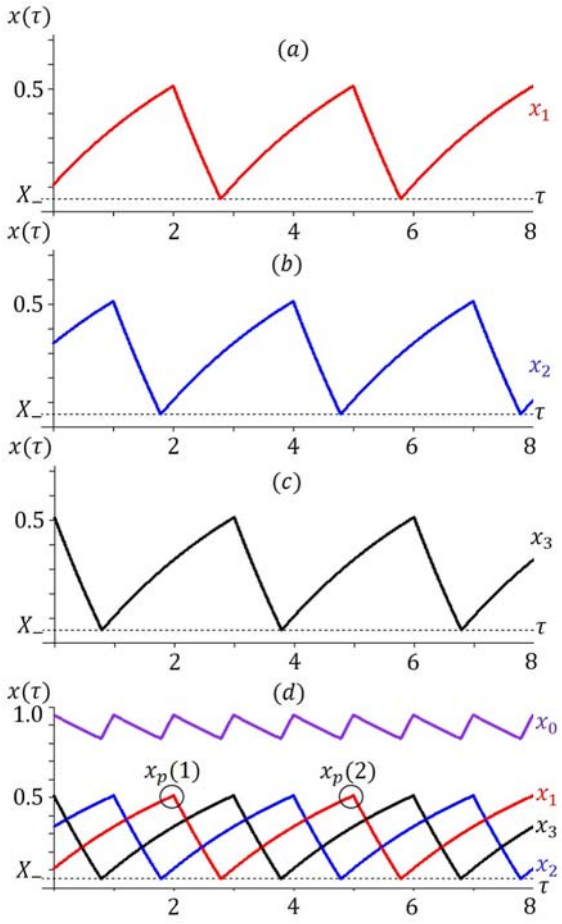

Figure 4: Typical waveforms. (a) Waveform of x_1 ($b_1 = 0.5$). (b) Waveform of x_2 ($b_2 = 0.5$). (c) Waveform of x_3 ($b_3 = 0.5$). (d) Waveform of 3-SYN ($b_1 = b_2 = b_3 = 0.5$)

3. Stability of N-phase synchronization

Here we define the N-phase synchronization (N-SYN) for $N = 3$. Let $x = (x_1, \ldots, x_N)$. x is said to be N-SYN if

$$\begin{aligned} &x(\tau + 3) = x(\tau) \\ &x_2(\tau) = x_1(\tau + 1),\ x_3(\tau) = x_2(\tau + 1) \text{ or} \\ &x_3(\tau) = x_1(\tau + 1),\ x_2(\tau) = x_3(\tau + 1) \end{aligned} \tag{7}$$

Conditions to be N-SYN is $b_1 = b_2 = b_3 = b$. The N-SYN is stable if

$$Df_N(a, b) \equiv \left| \frac{X_- - P_1}{X_- + P_2} e^{-\alpha N} \right| < 1 \tag{8}$$

where $P_1 = a/\gamma > 0$, $P_2 = b/\gamma > 0$, $0 < X_- < P_1$.

Fig. 5 and 6 show the stable factor Df for $N = 3$ and $N = 2$, respectively. Fig. 7 (a) shows a waveform of 3-SYN with input current. In Figs. 5 and 6, the bifurcation diagram is given by peak of x_1, indicated by x_p in Fig. 7 (a). In Fig. 5, 3-SYN is stable (unstable) for $b > b_p$ ($b < b_p$) where $Df_3(0.3, b_p) = 1$. In Fig. 6, 2-SYN is stable (unstable) for $b > b_q$ ($b < b_q$) where $Df_2(0.3, b_q) = 1$. Note that $b_p < b_q$.

That is, both 3-SYN and 2-SYN are stable for $b > b_q$. 3-SYN is stable and 2-SYN is unstable for $b_q > b > b_p$. Both 3-SYN and 2-SYN are unstable for $b_p > b$.

Here we assume that an accident occurs and the third converter is broken in the case of where 3-SYN is stable. The system of 3 converters is changed into that of 2 converters. If $b > b_q$ then 2-SYN is stable after the accident as shown in Fig. 7 (a') where ripple is reduced after the accident. If $b_q > b > b_p$ then 2-SYN is unstable after the accident as shown in Fig. 7 (b'). If $b_p > b$ then unstable 3-SYN is changed into hyperchaos as shown in Fig. 7 (c'). In order to consider the dynamics, we introduce the Lissajous figure as shown in Fig. 8. The Lorenz plot suggests complicated dynamics. The failed converter can exhibit interesting chaotic phenomena as shown in Fig. 7 (c') and Fig. 8 (c).

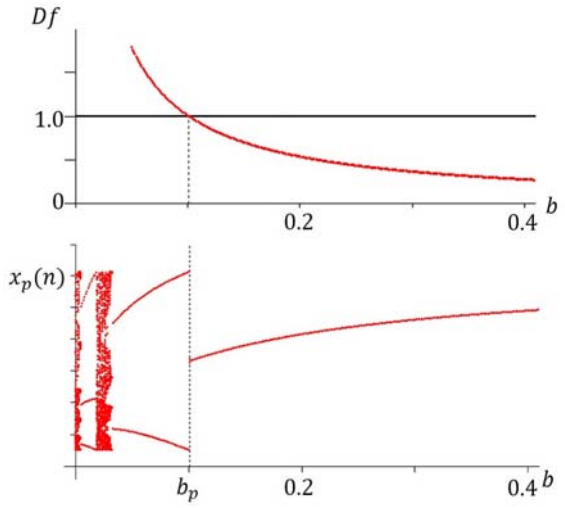

Figure 5: Bifurcation diagram from/to 3-SYN. ($a = 0.3$, $\gamma = 0.3$)

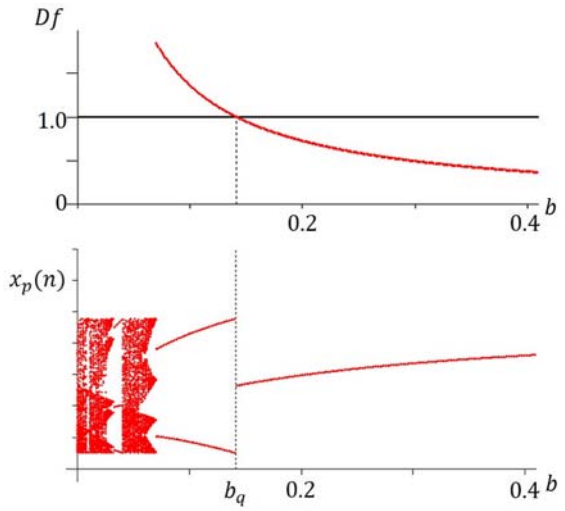

Figure 6: Bifurcation diagram from/to 2-SYN. ($a = 0.3$, $\gamma = 0.3$)

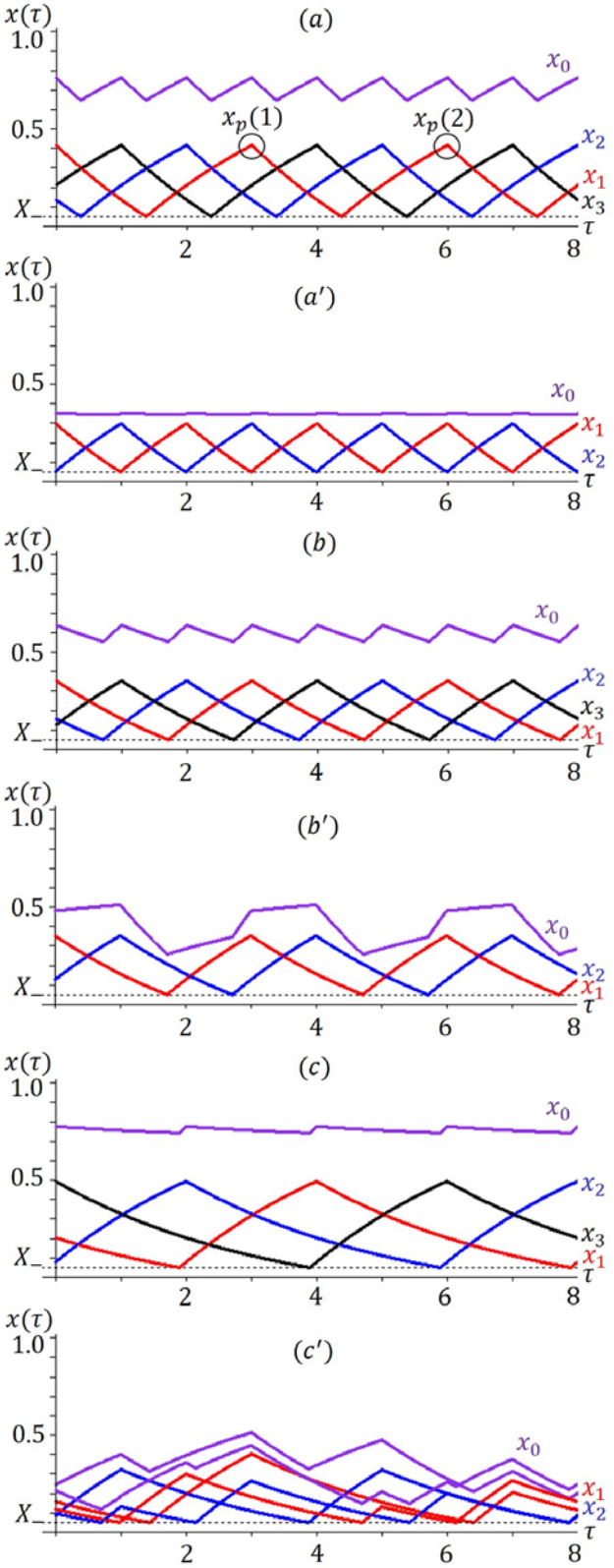

Figure 7: Typical waveforms ($a = 0.3$, $\gamma = 0.3$) (a) Stable 3-SYN and input current $b = 0.20$ before the accident (a') Stable 2-SYN $b = 0.20$ after the accident. (b) Stable 3-SYN $b = 0.12$ (b') Unstable 2-SYN $b = 0.12$. (c) Unstable 3-SYN $b = 0.045$ (c') Hyperchaos $b = 0.045$.

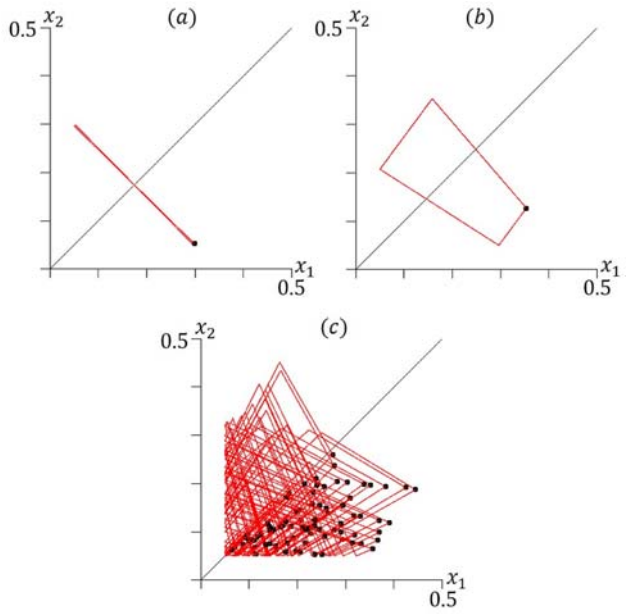

Figure 8: Lissajous figure of current waveform. (a) to (c) corresponds to the Fig. 7 (a') to (c'), respectively. Black dots denote the Lorenz plot at which x_1 is the local maximum.

4. Conclusion

Introducing a simple PWL model of paralleled boost converters. Stability of N-SYN and fault-tolerance have been considered in this paper. It is confirmed that the WTA-switching rule can preserve N-SYN after the accident in some parameter a range. Future problems includes more detailed analysis of stability, ripple characteristic, and power efficiency. Now we are preparing laboratory experiments for confirmation of typical phenomena.

References

[1] T. Saito, T. Kabe, Y. Ishikawa, Y. Matsuoka and H. Torikai, Piecewise constant switched dynamical systems in power electronics, Int'l J. of Bifurcation and Chaos, 17, 10, pp. 3373-3386, 2007.

[2] T. Saito and D. Kimura, Synchronization and Hyperchaos in Switched Dynamical Systems based on Parallel Buck Converters, IEICE Trans. Fundamentals, E92-A, 8, pp. 2061-2066, 2009.

[3] Y. Murata and T. Saito, Synchronization and chaos in a coupled system of two boost converters, Technical report, IEICE, NLP2015-4, 2015.

[4] S. Banerjee and G. C. Verghese, eds., Nonlinear Phenomena in Power Electronics: Attractors, Bifurcations, Chaos, and Nonlinear Control, IEEE Press, 2001.

[5] R. Giral and L. Murtinez-Salamero, Interleaved converters operation based on CMC, IEEE Trans. Power Electron., 14, 4, pp. 643-652, 1999.

[6] X. Zhou, P. Xu and F. C. Lee, A novel current-sharing control technique for low-voltage high-current voltage regulator module applications, IEEE Trans. Power Electron., 15, 6, pp. 1153-1162, 2000.

[7] H. Renaudineau, A. Houari, A. Shahin, J. -P. Martin, S. Pierfederici, F. Meibody-Tabar and B. Gerardin, Efficiency Optimization Through Current-Sharing for Paralleled DC-DC Boost Converters With Parameter Estimation, IEEE Trans. Power Electron., 29, 2, pp. 759-767, 2014.

[8] S. Chae, Y. Song, S. Park, and H. Jeong, Digital Current Sharing Method for Parallel Interleaved DC-DC Converters Using Input Ripple Voltage, IEEE Trans. Ind. Informat., 8, 3, pp. 536-544, 2012.

[9] T. Ohata, S. Kirikawa and T. Saito, Fault Tolerance of Simplified Parallel Power Converters with Current Sharing Function, Proc. IEEE APCCAS, pp. 104-107, 2012.

[10] K. S. Tey and S. Mekhilef, Modified Incremental Conductance Algorithm for Photovoltaic System Under Partial Shading Conditions and Load Variation, IEEE Trans. Ind. Electron., 61, 10, pp. 5384-5392, 2014.

[11] Y. Wang, Y. Li, and X. Ruan, High-Accuracy and Fast-Speed MPPT Methods for PV String Under Partially Shaded Conditions IEEE Trans. Ind. Electron., 63, 1, pp. 235-245, 2016.